

Research Article

Methodology for the Holistic Design of Format-Flexible Lithium-Ion Battery Systems

Julia C. Gandert ¹, **Raphael Mühlfort**¹, **Philip Müller-Welt**², **Daniel Schall**³,
Adrian Schmidt⁴, **Sebastian Schuhmann**⁵, **Philipp Seegert**¹, **Niklas Weber**⁶, **Yunying Zeng**²,
Thomas Wetzel¹ and **Sabine Paarmann**¹

¹*Institute of Thermal Process Engineering (TVT), Karlsruhe Institute of Technology (KIT), 76131 Karlsruhe, Germany*

²*Institute of Product Engineering (IPEK), Karlsruhe Institute of Technology (KIT), 76131 Karlsruhe, Germany*

³*Institute of Electrical Engineering (ETI), Karlsruhe Institute of Technology (KIT), 76131 Karlsruhe, Germany*

⁴*Institute of Applied Materials-Electrochemical Technologies (IAM-ET), Karlsruhe Institute of Technology (KIT), 76131 Karlsruhe, Germany*

⁵*Fraunhofer Institute for Chemical Technology (ICT), 76327 Pfinztal, Germany*

⁶*Institute of Mechanical Process Engineering and Mechanics (MVM), Karlsruhe Institute of Technology (KIT), 76131 Karlsruhe, Germany*

Correspondence should be addressed to Julia C. Gandert; julia.gandert@kit.edu

Received 22 September 2023; Revised 6 December 2023; Accepted 16 December 2023; Published 18 January 2024

Academic Editor: Amar Patil

Copyright © 2024 Julia C. Gandert et al. This is an open access article distributed under the Creative Commons Attribution License, which permits unrestricted use, distribution, and reproduction in any medium, provided the original work is properly cited.

Most battery cells are developed according to a standard design and optimized regarding their electrical properties. However, firstly, there is a demand for an individual cell design adapted to the application. Secondly, additional properties, for example, thermal and mechanical, are decisive for the cell behavior and should be considered in the overall design. Therefore, the present work introduces a model-based development tool for the holistic design of format-flexible battery cells, which are optimized for their future application, allowing for different cell geometries within one battery system. The different approaches and simulation models for the single design steps are presented, and the prediction of the electrochemical, electrical, and thermal behaviors of the cell and whole battery system is described. A key aspect here is the appropriate interconnection of the single models in a way that helps to narrow down the multitude of interacting parameters in a systematic manner and, thus, makes a holistic design possible. In a last step, the functionality of the tool is shown in a case study by means of an e-bike battery pack.

1. Introduction

Lithium-ion batteries are of utmost importance in the sector of mobile applications, such as power tools, smartphones, or even automobiles. While a wide range of research is conducted on the development and investigation of new cell chemistries, the basic principle of the battery cells has not changed and lithium-ion batteries are expected to be highly relevant in the future [1].

The typical shapes of lithium-ion battery cells comprise standard formats, either cylindrical (e.g., 18650 and 4680), or

rectangular prismatic or pouch cells. In the majority of cases, the application is then built around this standard battery.

Following this logic, there have been new approaches for the optimization of battery cells, modules, and whole systems. By varying the thickness and porosity of the electrodes, single cells are optimized for high-energy and high-power applications [2]. Furthermore, the impact of the inner cell structure on the whole system behavior was investigated, and an optimization on the system level was allowed [3]. With a similar approach adopting a cell-module model, Epp and Sauer aimed to optimize a unified cell format to

significantly reduce the costs of batteries for electric vehicles by lowering their production costs due to high production quantities [4]. On a pack level, approaches for the battery system optimization with 18650 cylindrical standard cells [5] and prismatic hardcase cells [6] are known.

Another approach of the automobile industry to integrate the battery into the vehicle better and boost the energy density is the cell-to-pack or cell-to-chassis technology [7]. The standard cell format is accepted there without question. As an existing installation space is rarely the exact multiple of a standard cell shape, cells with several well-adapted formats enable it to be filled more effectively. We call these cells format-flexible. "Flexible" does not refer to deformable cells that can be bent even during operation, as described by Ha et al. [8]. Instead, the term "flexible" refers here to the design and production steps needed to achieve the variable, adaptive cell geometries. Those format-flexible cells have the potential to significantly increase the energy density at application level. This potential is currently only being leveraged in a few applications of consumer electronics such as the L-shaped battery of recent iPhones [9, 10] and the hexagonal battery developed by LG for smartwatches (Figure 1(a)).

An analogy can be drawn historically with the development of the gasoline tank in the combustion vehicle. The first models simply had a large cylindrical tank that had to be accommodated in or on the vehicle (Figure 1(b)). Today, by contrast, the tank is manufactured by injection molding and fills every available nook and cranny in a predefined design space, thus reaching an optimum in fulfilling concurrent requirements in the overall system design (Figure 1(c)). A similar development is feasible for the battery in the medium term.

The battery production in European research institutions and industry is already, although slowly, experiencing a transition from the exclusively mass production of standard cells towards the additional operation of more agile production plants, which enable the profitable manufacturing of lower batch sizes and a more flexible choice of materials and cell shapes [11–16].

An application-specific design of the cells and the battery system is needed to make use of the advantages of such agile production systems and the format-flexible cells produced therein. This publication provides an overview of the distinct steps and factors to be considered in the design process for battery systems based on format-flexible cells. In order to reach ideal energy and power densities, a tool is created that supports the developer in the design of battery systems containing format-flexible cells. Therefore, it has to be easy to use and enable a fast design of the holistically optimized battery system. This tool will be introduced as the result of this work.

In contrast to battery systems based on standard cell formats, those designed with this innovative design tool do not only reach the electrical specifications and safety standards requested but also include thermal and mechanical optimization steps in a holistic battery design. Moreover, customer- or application-oriented optimization is implemented through flexible prioritization and the weighting of target variables, such as costs, installation space, and energy density.

The design of an e-bike battery pack is introduced in detail as a case study at the end of this work to give insight into the use of this tool.

2. Methodology of the Design Process

The newly gained flexibility of cell sizes and geometries and their combination even within a single battery system allows for new options regarding system development. However, it also needs an advanced design process to systematically make use of the different sizes, shapes, and internal structures of the cells. The combined consideration of the electrical, thermal, mechanical, and safety-related boundary conditions entails a complex solution space [21].

The fundamental goal of the design process presented here is to define the optimal battery system for any given application. Starting with the cell chemistry, through the internal structure of the individual cell and the circuit topology, to the cooling system and safety components, there are countless variables and endless possible combinations for the final battery. In order to manage this variability, it is essential to conduct a prescreening of viable combinations that align with specific requirements of the target application. Accordingly, the infinite number of combinations in a more or less continuous design space has been replaced by a finite number of discrete parameter combinations that maintain the flexibility desired, while limiting the complexity and enabling the efficient design process required. The result of this reduction process is called a modular toolkit and will be described in due course.

Moreover, the approach of product-production code-sign is pursued [11], especially focusing on agile production. On the one hand, this leads to some limitations in the design space, but on the other hand, this approach allows for an optimal utilization of the agile production line and enables the validation of the design tool with the cells produced. Pouch bags as casing constitute a far higher flexibility for the production than the rigid housing of cylindrical and prismatic cells [9]; therefore, pouch cells are the subject of this work. Although material variation is highly relevant for battery flexibility, it also comes with a great effort to parameterize the models accordingly. In this work, we looked at graphite/NMC622 as the exemplary cell chemistry.

In the following, we discuss the single steps of the design process we performed for the dimensioning of application-oriented battery systems. The sequence of those steps is schematically depicted in Figure 2, which also represents the content structure of this section. Hereby, a simplified linear approach is shown. The objective of the design tool developed is to manage the process with as few iterations as possible. However, it is expected that iteration loops between and within the single steps are necessary to approach an optimal design of the battery system during the development phase until the verification of the final software tool.

The design process can be divided into the following steps with the enumeration corresponding to Figure 2:



FIGURE 1: (a) Examples of application-oriented, format-flexible cells in consumer electronics: battery of the iPhone 12 [17] and hexagonal battery by LG Chem [18] for use in smart watches. Comparison of (b) the cylindrical tank used around 1915 [19] and (c) the tank in recent automobiles [20] (reproduced with permission, Copyright 2004 Elsevier).

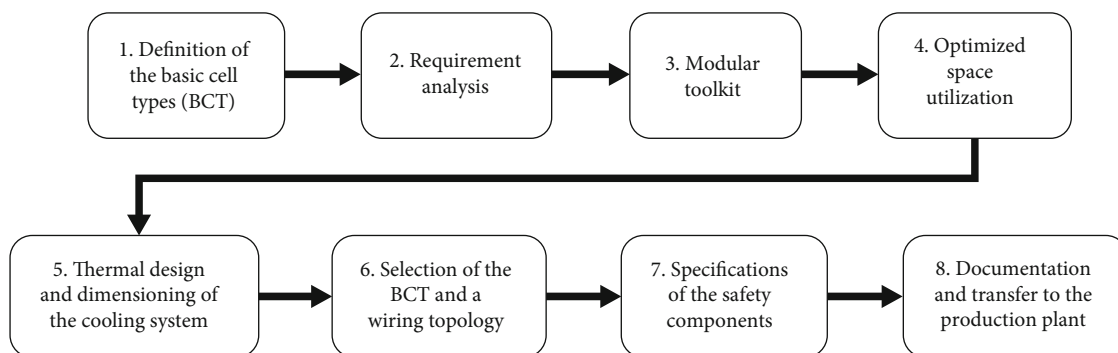


FIGURE 2: Flow chart of the battery system design process.

- (1) Definition of the basic cell types (BCTs): five BCTs are defined before the actual design process. Their chemistry is predefined, while their internal structure varies and is electrically optimized to cover a wide range between high-power and high-energy systems
- (2) Requirement analysis: a detailed specification of the requirements is needed for a truly customized battery system. Therefore, the design procedure starts with an analysis of the application regarded

- (3) Modular toolkit: knowing the properties required, such as the capacity, power capability, and available installation space, the toolkit is utilized for the preselection of possible safety, wiring, and cooling options
- (4) Optimized space utilization: the format flexibility of the cells regarding the outer dimensions takes effect during the filling of the installation spaces. The size and shape of the cells are varied freely between certain limits to achieve a high energy and power density on a system level
- (5) Thermal design and dimensioning of the cooling system: with the knowledge of the inner and outer dimensions of the cells, the thermal model is parameterized. Firstly, this is used for the simulation and dimensioning of the cooling system. Secondly, its results are used to parameterize a simplified thermal model for evaluating the thermal cell behavior within the next step
- (6) Selection of the BCT and a wiring topology: during the electrical simulation of the whole battery system, the best possible BCT as well as the combination of series and parallel connections (electrical topology) and optimal electrical connection elements and welding methods are chosen
- (7) Dimensioning of the safety devices: in the last step of the actual dimensioning, a simulation of the thermal runaway and thermal propagation within the battery module is conducted and suitable safety precautions are selected
- (8) Documentation and transfer to the production plant: lastly, the data of the optimized battery system gained during the whole design process is submitted to the database of the production system

Each step requires the previously generated information and adds further data to the design; thus, a shared database is key to the process. It enables data integration all the way down to the production system. As the core of the whole design tool is programmed in MATLAB®, a MATLAB® structure was chosen for the storage of the system parameters identified. The buildup of the data structure is shown in Figure 3. The project is hereby divided into five possible arrangements of the cells and modules within the installation space. The system capacity, the number of modules, and their suggested connection are specified for each arrangement. An arrangement typically comprises multiple modules, which, in turn, consist of the individual cells themselves. Within the cell partition, the inner and outer dimensions as well as the electrical and thermal properties are specified. Furthermore, each module has a partition for the cooling system and a specification of the safety devices.

2.1. Definition of the Basic Cell Types. As a preliminary design step, the definition of the BCTs is not conducted for the design of every single battery system. It is, instead, only carried out once for each cell chemistry to be considered.

The outer dimensions are varied only during the space filling of the design process for a specific application.

A broad variation of the inner cell structure from high-power to high-energy cells is needed to cover a wide range of applications. At the same time, the number of variations has to be limited to ensure manageability. Therefore, five so-called BCTs were defined in this work, covering the range from high-power to high-energy setup. Fixed parameters, hereby, are the cell chemistry, particle size distribution of the active material, solid material composition of the electrode coating, and the layer thickness of the current collectors and separator. The main variation is conducted through the porosity and the coating thickness of the anode and cathode.

A multiphysical modelling approach was used to predict the cell performance while accounting for the nonlinear interdependencies of internal cell processes. Therefore, the aforementioned limitations, influences, and correlations were implemented into the multiscale multidomain model described by Schmidt et al. [22], which allowed for an optimization of the inner structure for different power requirements. The BCTs derived for an exemplary graphite/NMC622 cell chemistry are depicted in Figure 4. The power densities are, hereby, referred to a pulse length of 2 min.

For the specification of the basic cell types, the layer thicknesses, porosities, and subordinate microstructure parameters were varied considering the boundaries prescribed by the production system. Hereby, the feasible porosities, coating thicknesses, and overall electrical properties of the electrodes are determined by the coating, drying, and calendaring step and their realization within the production plant [23]. The production boundaries referred to in this work are given in Table S1 in the Supplementary Information. The thickness of the current collector foils was kept constant to ensure manufacturability. Additional parameters, such as the separator thickness, separator porosity, and conductive additives of the cathode, were kept constant, while the electrical conductivity and tortuosity of the electrodes were calculated by correlation functions, as described in Laue et al. [24]. This allows for the tuning of the electrical performance of the battery cell, such as the internal resistances and cell capacities. High-energy cells are defined by high coating thicknesses and low porosities. Consequently, high active material fractions and energy densities can be reached. High-power cells with high current demands instead have thinner layers of active material and high porosities to reduce the internal cell resistance, limit the heat release during operation, and improve the heat transfer out of the cell [25].

The porosity is varied between 20% and 35% for the anode and from 20% to 30% for the cathode, while one coating layer thickness goes from approx. 130 μm for the high-energy cell to 35 μm for the high-power cell with very similar values for both electrodes. Due to the varying layer thicknesses between the five BCTs, different numbers of unit cells consisting of anode–separator–cathode are stacked to reach approximately the same overall stack thicknesses.

As the high-resolution multiscale multidomain model is too slow to be implemented in the subsequent steps of the

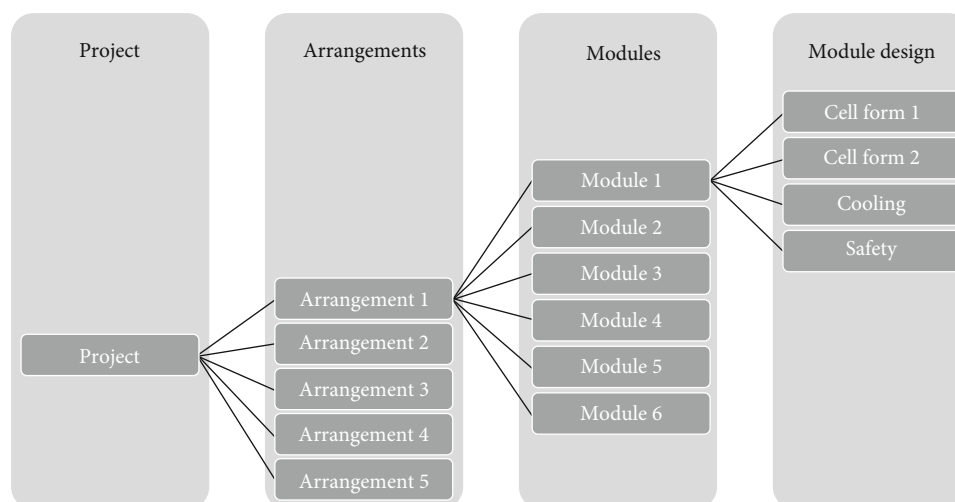


FIGURE 3: Schematic depiction of the subdivision of the MATLAB® structure. A similar partitioning can be made for the arrangements 2 to 5 and the modules 2 to 6, respectively.

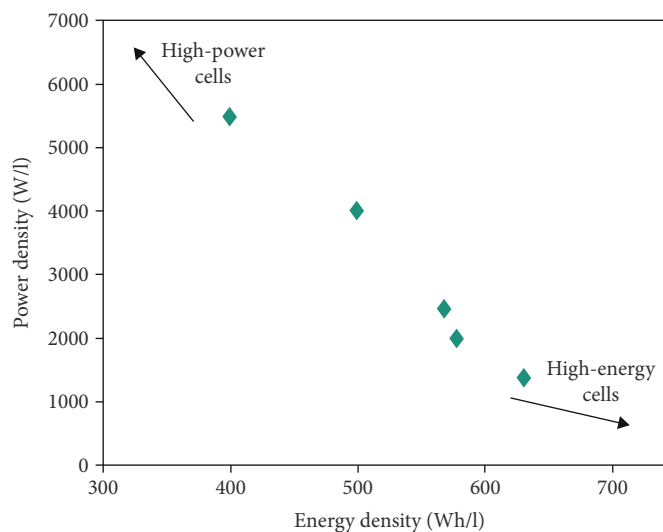


FIGURE 4: The Ragone plot of the five basic cell types for a graphite/NMC622 cell chemistry identified in this work.

design process, it is used to parameterize a simplified equivalent circuit model of the type R-RC-RC. This model runs much faster, while still replicating the cell voltage response with a mean squared error of less than 10 mV when simulating a dynamic profile of 3000 s. Thus, it can be used by the thermal simulation to estimate the heat generation and the simulation of the different wiring topologies to estimate the voltage and state of charge (SOC) during operation.

These BCTs build the foundation for the design of the battery systems for different applications, allowing an easy and discrete variation between high-power and high-energy cells and the space in between.

2.2. Requirement Analysis. As the requirements for a battery system depend greatly on the application, they have to be specified in the first step by or with the help of a potential customer. A questionnaire was developed to assist in and stream-

line this specification analysis. It is divided into three sections: the essential requirements, optional information about an existing reference product, and additional specifications.

The most important requirements for the battery system design include the system voltage, power demanded, minimum capacity, and a computer-aided design (CAD) file of the installation space.

Furthermore, similar information about the reference product, such as the capacity, costs, and the cell type used in case of using standard cells according to the German Association of the Automotive Industry, is interesting for a comparison and assessment of the system achieved with the new design tool.

Additional information is, for example, preferences regarding the cooling medium, the housing material, or electrical and thermal safety devices used.

The complete questionnaire is given in the Supplementary Information of this paper (available here).

2.3. Modular Toolkit. Müller-Welt et al. [26] developed a simplified methodology to handle the complexity of the design process. They compiled a toolkit which assembles an initial system configuration—in our case, of the battery system—out of many different subsystems by making choices for each of them individually. Since the design tool is intended to cover a large number of different systems and applications, it is reasonable to exclude components and combinations that are not feasible for a given application in advance.

While looking at all the different subsystems—safety concept, cooling concept, electrical cell selection, and battery management system (BMS)—with their multiple second level subsystems, it is decided which options are possible and which one is preferable for certain applications. As an example, we take a closer look at the impact of the specific application regarding the choice in the cooling concept. Hereby, an air-cooled system is not suitable for an automotive application with high power and, therefore, high cooling demands. However, for several applications, such as drills, fluid cooling is not an option due to space and weight considerations. Further distinctions are made for power tools and home appliances, as it makes a big difference, whether the device is in continuous or only occasional use. Occasional use, for example, allows for relaxation phases and cooling down between utilization periods. Furthermore, the impact of calendar aging is far more important for the occasional user in comparison to cyclic aging, making cooling during operation less important.

It needs to be considered during preselection whether all of the subsystems might be interconnected or exclude each other. Heat spreaders for fast heat removal and thermal barriers for the prevention of thermal runaway propagation between the cells, for example, frequently pose a conflict of goals. Such dependencies were taken into account during the development of the toolkit. Hereby, every combination was assessed separately. Thus, the implementation of the toolkit takes up a lot of thought and effort but accelerates the proper dimensioning significantly.

All the choices can be made due to either technical or economic reasons. This implies a possible prioritization towards different aspects, such as costs, energy density, or weight, when putting together the battery system from the different subsystems. Thus, viable concepts of the subsystems are identified that most closely align with the prioritization chosen. This way, a foundation to effectively carry out the subsequent analysis and design process is established.

A more detailed description of this approach is given by Müller-Welt et al. [26].

In the long run, the currently defined criteria for prescreening can be modified and the applicability of the tool can be extended as desired.

2.4. Optimized Space Utilization. Each application and product has a unique design in which the battery should be integrated even if the space available is small or has a complicated shape. Thus, the main goal of this step is to fill the available space with battery cells in a way that maximizes the volumetric energy and power density of the battery system. At the same

time, the system voltage demanded and possible wiring topologies are considered. Hereby, it is important to take not only the volume of the cells into account but also the space needed for additional components, such as the clamping system, electrical connectors, cooling system, and thermal barriers.

The size of the cells and modules needs to be specified to reach an optimized space utilization. The parameter sets obtained for the different cell types allow a broad variation of the outer dimensions of the battery cells. However, the cell thickness is a multitude of the unit cell thickness and has to stay below the maximum stacking height, which is, in this case, dictated by the production line. By contrast, the length and width of the battery cells can be varied freely and are only restricted by the upper and lower limitations of the dimensions prescribed by the production plant.

Restrictions for the wiring of the cells and modules have already been considered during the space-filling process. The basic rules are applied so that only cells with equal internal resistances are connected in parallel and only cells or modules with the same capacity are connected in series. Apart from that, it was specified that all cells within a system are of the same BCT and, therefore, have the same inner structure. This approach allows an easier dimensioning and connection of the cells by demanding that the cell volumes within a system are always a multiple in size. As the nominal capacity of the cells is estimated by the volumetric energy density on an electrode level, which is different for each cell type, scaling in cell size coincides with a scaling in capacity.

With these premises in terms of thicknesses and size ratios, the installation space is filled with five different arrangements, one for each of the five different cell types. Those are compared later during the selection of a wiring topology, and the best option is chosen.

The module structure is defined prior to the actual space filling. It depends on the selected cooling, safety concept, number of cells per module, and thickness of a single cell which varies between the cell types and can be further adjusted if necessary.

With the knowledge of the target module thickness, the virtual installation space is scanned to determine the maximum possible length and width of the module. The modules can then be automatically arranged within the space available, and the preferential orientation of the modules within the battery system is determined. In case of big differences in the length and width of the modules, a parallel connection of cells within a module is considered in addition to a pure series connection. In this way, the requirement of equal capacities or voltages depending on the further connection of the modules is fulfilled.

The outer dimensions of the cells also define the size of the current collector tabs. The largest geometrically possible and physically available tabs are used for simplicity during the production process. In the future, however, it is also conceivable to scale the width—or, more specifically, the cross-section—of the tabs with the volume or maximum current of the cells.

It is crucial during the virtual space filling with modules to already consider possible wiring options. The modules may be connected either in parallel or in series. The choice

of the best option depends on many factors, such as the cell and module quantity, the module voltage level, the distance within the installation space, and the voltage required of the whole battery system [27].

The authors refer to the publication by Müller-Welt et al. [27] for a detailed description of the methodology used for the space filling.

The outputs of the space-filling step are five arrangements—one for each of the BCTs—and the relevant information about nominal capacity and nominal voltage of the battery system, number of modules, number of cells per module, and external and internal dimensions of the different cells.

2.5. Thermal Design and Dimensioning of the Cooling System. The design tool comprises a thermal cell model and cooling optimization for the system as the thermal cell behavior and especially the heat removal from the cells impact the electrical performance of the cells [28] and the battery system as a whole significantly. Hereby, an acceptable application-specific temperature range and adequately low thermal gradients within and between the cells during operation are ensured. The goal here is to reach low and homogeneous aging and prevent critical temperature rises potentially causing a thermal runaway. Different cooling scenarios, such as bottom cooling with and without heat spreaders between the cells [29, 30], fluid flow cooling plates between the cells [31, 32], fin air cooling [33], or a passive system without any active measures, are considered to meet the needs of a variety of applications. With the modular toolkit (Section 2.3), a preselection of the cooling system is made for the specific application based on the heat generation expected and the priorities specified for the relevant applications. A detailed simulation is only conducted for the most promising cooling concepts. In the first step, default values included in the model are used for variables, such as volume flow rate, number of channels, or fin length, which can be further adjusted if needed.

All thermal electrode properties show a strong dependency on the volume fraction of the different components and, thus, also the layer thicknesses and porosities of the electrodes. This is why the parameterization of the thermal model is conducted individually for all the five arrangements obtained during the space-filling step, leading to a cell type-specific and thickness-dependent parameterization of the model concerning the thermal material properties. Mean values of the density and specific heat capacity of the cell stack are calculated following a volumetric and mass-specific averaging, respectively [34]. Regarding the effective thermal conductivity of the battery stack, it is distinguished between the in-plane thermal conductivity and through-plane thermal conductivity, which are calculated from a parallel and series connection of the single components, respectively [35]. Furthermore, the thermal mass of the peripheral components, such as clamping and safety devices as well as the cooling plates and fluid themselves, is considered as it significantly influences the speed of temperature changes during operation.

Using those parameters, a detailed simulation of a single cell is conducted with a finite volume method model. The

results can then be used to parameterize a simplified zero-dimensional thermal model and increase the calculation speed for use within the electrical wiring simulation in the following design step. Hereby, it is important for the prediction of the temperature gradients between the single cells of one module to take into account the connections between cells in the form of compression pads, heat spreaders, and thermal barriers as well as electrical connectors, such as bus bars. However, the most important variable is the heat transport out of the system via the cooling system and further linkages to the environment.

The decisive output parameters to evaluate the cooling system are the maximum cell temperature and the maximum temperature difference within a cell and between the cells of a module. How much importance is given to these values depends greatly on the costs pursued and operating conditions of the application. All these boundary conditions provide different temperature thresholds for the simulation.

In the end, the final parameterization of the cooling system, which reached the set temperature goals, and the parameters for the simplified model describing the thermal cell behavior for the electrical simulation are saved within the database. The simplified model, hereby, provides the thermal mass of the cells and the peripheral components as well as heat transport coefficients towards the environment (air), the periphery (housing and cooling system), and the cooling fluid and cell-to-cell heat transport coefficients. All the coefficients are referred to the caloric mean temperature of the cells and other components to avoid multidimensional simulation of the thermal behavior in the electrical model.

Some iteration loops through the detailed thermal simulation, the parameterization of the simplified thermal model, and the electrical simulation might be needed to reach coherent results of the different models.

2.6. Selection of the Cell Type and a Wiring Topology. While the preceding steps investigated the possibilities and behaviors of all five BCTs, a choice of the inner cell structure is finally made in this step. Which cell type is most suitable depends greatly on the power demanded by the application and the circuit connection implemented. Thus, the options for the parallel and series connection of the single cells and whole modules proposed during the space filling for the different arrangements are taken into detailed consideration here and undergo an electrical module simulation. Hereby, the electrical behavior of the cells is modelled according to the equivalent circuit model, which is parameterized for the different cell types as described in Section 2.1. The temperature development and thermal gradients between the cells and modules are predicted by the simplified thermal model, which is described in detail in the previous section.

The goal of this step and the wiring chosen is the realization of uniform charge and discharge of the single cells and, thereby, the avoidance of deep discharge and inhomogeneous aging. Some assumptions are made for specifying the different configurations with cells connected in parallel and in series. We presume that the capacity of cells of the same BCT is linearly scalable with their stack volume, and the internal

resistance can be scaled with the reciprocal of the stack volume. Thereby, the usage of cells, which are a multitude in volume, greatly simplifies the wiring. Therefore, conventional solutions for the electrical battery management without active balancing or dynamic reconfigurability are sufficient [36]. Reconfigurable BMSs become relevant for more complex systems with strongly varying cell capacities and internal resistances. However, they are very elaborate and not always profitable, especially for small and cheap systems. That is why those active systems are not part of our approach.

With the results of the electrical simulation, the different topologies that fulfill the energy and power requirements are compared regarding the homogeneity of the SOC of the individual cells, the internal resistance of the system, and the costs of the electrical connectors and BMS components. These criteria are weighted in an objective function to choose the best BCT and electrical periphery. The weights in the objective function can be adapted according to the requirement analysis in Section 2.2.

2.7. Specification of the Safety Components. The components for a safe operation of the battery system are selected within the last step of the design process. The focus is on devices and materials for the prevention of thermal runaway of single cells and thermal runaway propagation to adjacent cells.

The safety of the battery packs designed is considered on various levels. At the cell level, each cell needs to be protected from any abusive conditions, including mechanical, electrical, and thermal stresses. In order to avoid potential thermal hazards, the cells are kept in a safe temperature range by the cooling system and the BMS developed in the previous design steps. The robust housing of the modules protects the cells from mechanical impacts. Thermal fuses or positive temperature coefficient devices can be used to detect and prevent thermal runaway. While thermal fuses interrupt the current flow by melting in case of a short circuit, positive temperature coefficient devices provide a highly temperature-dependent electrical resistance. In case of a significant temperature rise due to an external short circuit, they act as a high value resistor and drastically reduce the electric current [37].

However, even with all the safety measures noted, single cell thermal runaway can still occur in extreme situations. Therefore, at system level, the effects of thermal runaway have to be mitigated and thermal propagation has to be prevented. While safety valves are not required at the cell level due to the fragility of the pouch bags, valves are required at the system level to prevent pressure buildup and mechanical rupture of the housing [38].

Thermal barriers can be used for the prevention of thermal propagation [39, 40]. These barriers act as a thermal resistance to lower heat transfer between cells and modules. A three-dimensional finite volume method model was developed to evaluate the need and dimensions of this safety equipment, which combines thermal and chemical models, including the most significant decomposition reactions of the battery components. Accordingly, the temperature rise caused by exothermic reactions and the evolution of gaseous reaction products is simulated. Furthermore, the thermal

conduction between two cells and, thus, the thermal runaway propagation from one cell to another are replicated, and suitable measures can be taken to prevent this. The model was described in-depth by Weber et al. [41], including a detailed validation of the model.

To validate the model, thermal runaway experiments were conducted using cells with different capacities. Utilizing the temperature profiles recorded and an analysis of the gas phase released, the implemented reactions could be verified.

The results of the simulations of the battery systems designed indicate the number and thickness of thermal barriers needed. Again, several iteration loops may be needed for this.

2.8. Documentation and Transfer to the Production System. The results of the overall design tool are parameter sets for the whole product, i.e., defining the complete battery system. In addition to the outer geometry, inner structure, and electrical and thermal properties of the cells themselves, information on the wiring, cooling system, and safety devices is stored within a MATLAB® structure as shown in Figure 3.

This specification may then be transferred to the database and control system of the production plant, providing a bill of materials. This includes, for example, the active material mass, the number of electrode and separator sheets, their geometry, the size of the current collector tabs, and the electrolyte volume per cell. Within the database, correlations for the direct calculation from product parameters to process parameters can be specified which then allow the simple setting of the machines. In this way, the amount of the different components that is needed to produce the electrodes, cells, and, finally, the whole battery system can be predicted.

It is advantageous to make a visualization of the battery design available to the customers and supervisors of the production. Thus, a CAD model is used to enable a fast and automated depiction of the cell and module geometry with the established data of the whole process. Hereby, construction drawings of the cells are easily generated, and different system variations can be depicted without any additional expense. An example of this is given in the case study.

3. Discussion

Different underlying objectives were developed to evaluate the results of the design tool and its single process steps. The whole dimensioning is aimed at maximizing the energy and power density and minimizing the costs and system weight, always considering the aspects mentioned previously, such as space utilization, cooling conditions, inner cell structure, electrical topology, and safety concerns. Additionally, it is ensured that the systems can be disassembled easily. The objectives for the single steps are given in Figure 5. The optima of the individual steps can contradict each other. In such cases, the decision is not made automatically but by the operator of the tool.

As mentioned previously, we focus on the design and production of format-flexible pouch cells. An expansion towards cylindrical or prismatic cells is doubtful, as they

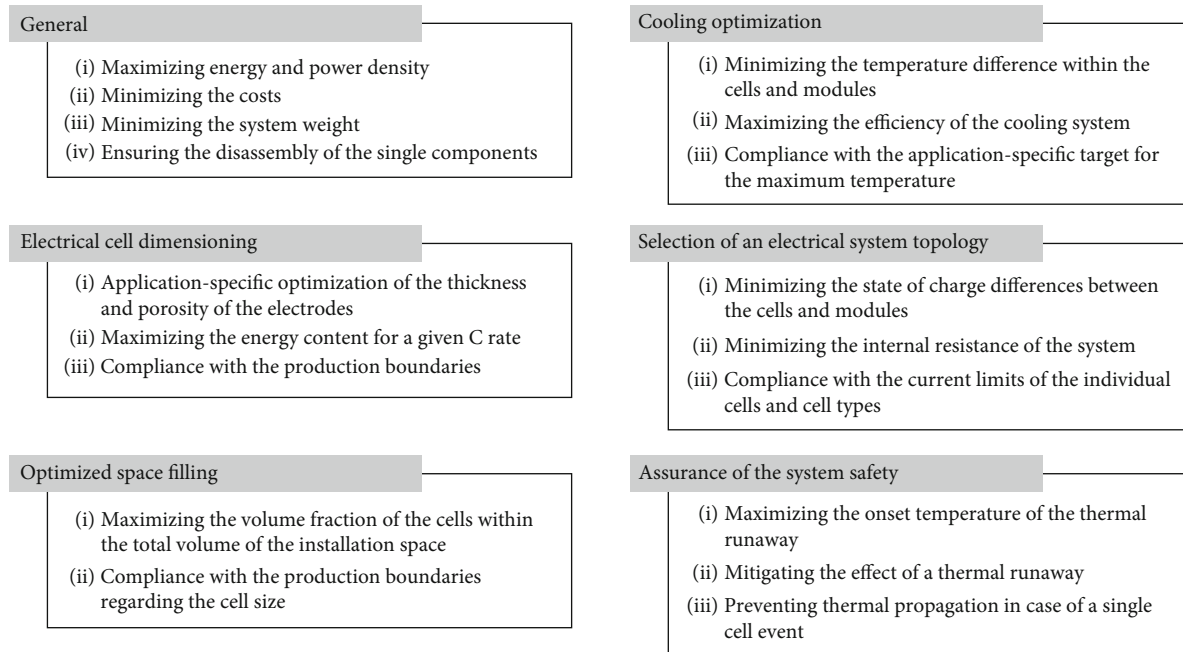


FIGURE 5: Objectives of the whole design process and the individual design steps.

are less suitable for the flexible production due to their rigid housings.

The design tool is not limited regarding cell size and edge lengths. The limitations considered in this work originate completely from the production plant regarded [11]. However, an expansion of the design tool for different production systems or changes with further development of the current system is conceivable.

So far, we only consider cells with straight edges in this work. Those include rectangular, triangular, and trapezoidal shapes. Cells with round edges could be incorporated into the design tool as well, though circular or ellipsoidal cells pose greater challenges on the production side.

We concentrate on only one cell chemistry for the development of this methodology due to the great effort of parameterizing the models. Nevertheless, the implementation of new cell chemistries is generally feasible and reasonable when new materials are compatible with the production system. In addition to those general expansion potentials, more arise in the individual design steps. A detailed explanation of those is provided in Figure 6.

The tool can be profitable to use for quite a lot of different applications by automating the whole design process.

4. Case Study

As an example, the BOSCH PowerTube 625 [42] e-bike battery pack was redesigned with the design tool presented here. The whole battery pack was disassembled and documented as CAD drawings as shown in Figure 7, to reach an in-depth understanding of the structure and integration of the current system as a reference.

The system consists of 50 cylindrical 18650 cells, connected in a 5p10s configuration with 5 cells in parallel build-

ing a module, and those 10 modules being connected in series. Hereby, a capacity of 16.7 Ah [42] is provided at a nominal voltage of 36 V resulting in a total energy content of approx. 625 Wh.

In this section, we follow the design process presented step by step.

4.1. Requirement Analysis. Following the disassembly of the battery pack and manufacturer's specifications, the requirements for the e-bike battery can be summarized as shown in Table 1.

Furthermore, exemplary load profiles for a light-load city tour and a more demanding mountain trip are given in Figure 8. Those are used as basis for the simulation of differences between the cells operated with the load profiles and the electrical design of the wiring topology.

The installation space is restricted by the outer dimensions of the original casing of the battery pack.

4.2. Modular Toolkit. Assuming the same cell chemistry and nominal cell voltage of 3.6 V, a series connection of ten cells is needed in the newly designed system as well to reach the system voltage demanded. The number of cells or modules connected in parallel depends on the total number of cells in the system and can only be defined during the space-filling step.

Based on basic boundary conditions, potential concepts from the construction kit developed are considered for the e-bike battery. Regarding the electrical concept, a cell-to-pack approach without modules and cells with counter tabs and bus bars is considered most suitable due to the space requirements. The initial analysis, furthermore, shows that the use of an active cooling system is not feasible for the application as the size and weight are highly restricted.

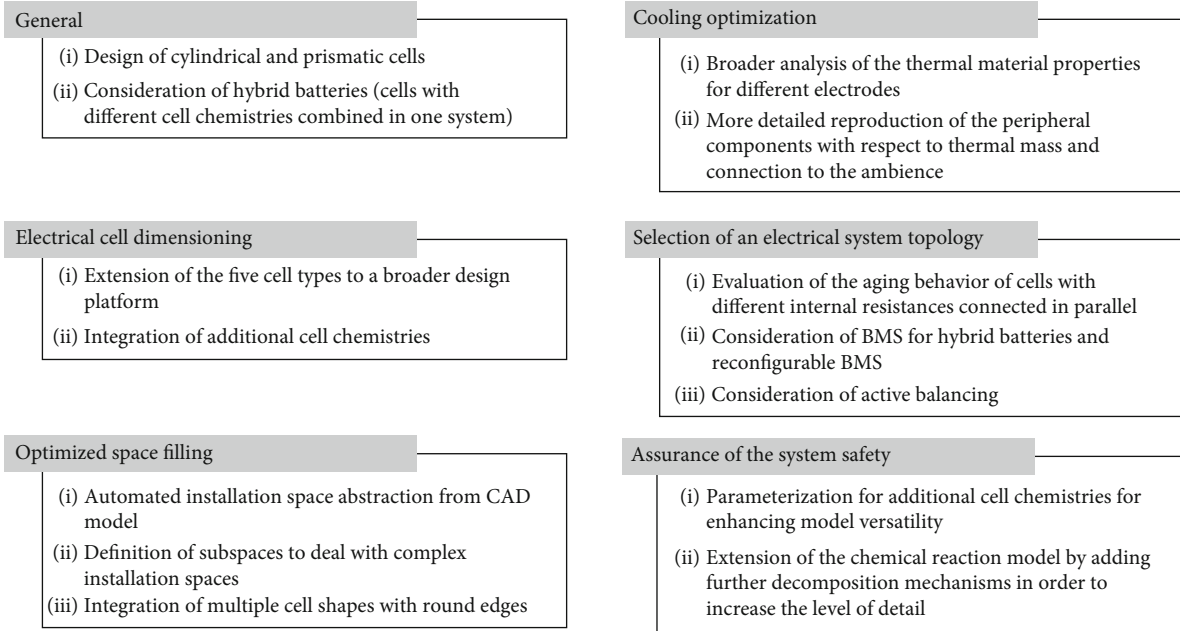


FIGURE 6: Expansion potential of the whole design process and the individual design steps.



FIGURE 7: Photographs of the original reference system built out of 18650 cylindrical cells and CAD images.

TABLE 1: General requirements for the e-bike system.

Requirement	Value
Capacity	>16.7 Ah
System voltage	36 V
Energy content	>625 Wh
Lifetime	500–1000 charge-discharge cycles until 70% state of health is reached
Maximum temperature	60 °C

Moreover, additional components, such as pumps and tanks, are not suitable for an e-bike application. As the load and heat generation are relatively low, the active cooling system may be dispensed. Regarding the safety concept, a basic BMS without active balancing is selected, while the use of thermal barriers is considered unnecessary.

4.3. *Optimized Space Utilization.* Due to the shape of the installation space, an octagonal cell geometry was chosen to reach an optimized space utilization in comparison to

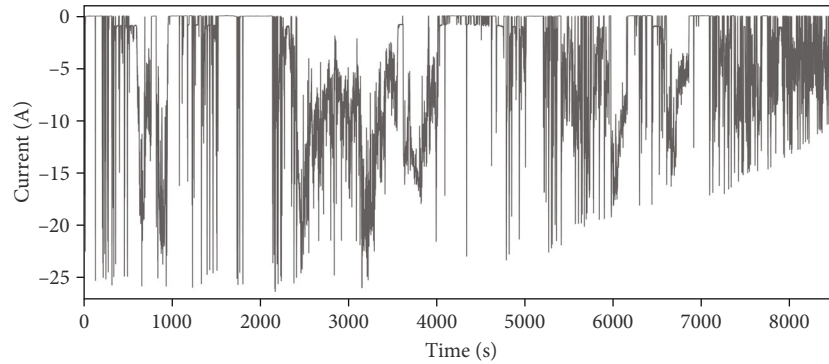


FIGURE 8: Load profile for the e-bike during a mountain trip. Negative currents represent discharge of the system.

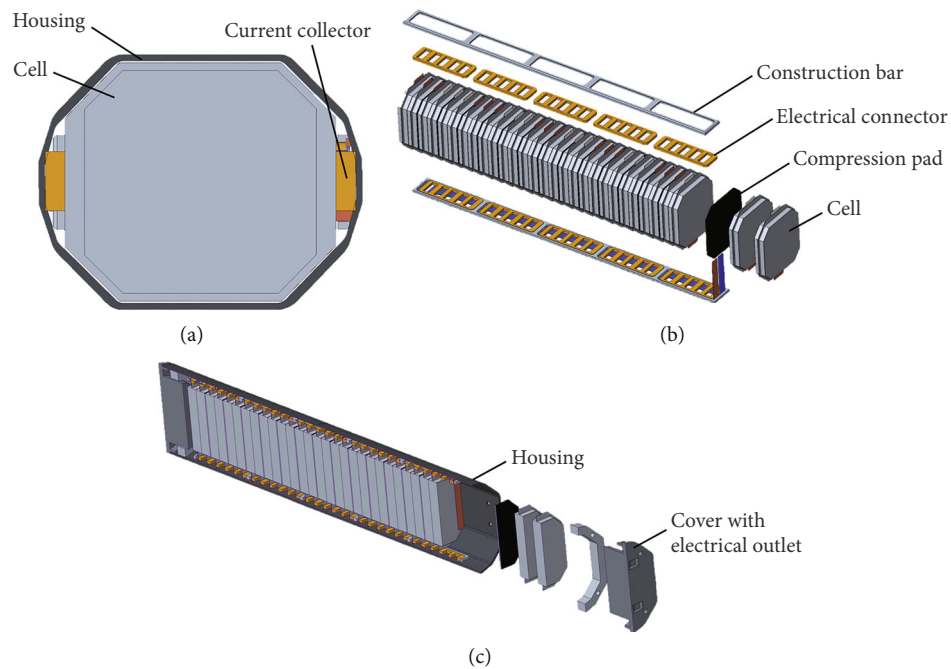


FIGURE 9: (a) Cross-section of the installation space and cell, (b) explosion drawing of the whole battery pack with electrical connectors, and (c) cross-section of the battery pack within the housing and cover.

rectangular cells and, thus, a higher volumetric energy and power density (see Figure 9). The constant cross-section of the installation space enables the use of only one cell form in the system, leading to a reduced complexity in the BMS in comparison to multiple cells with different cross-sections or volumes.

With a maximum allowed cell thickness of 12 mm, 30 cells can be fitted into the installation space, leading to a recommended wiring topology of 3p10s, which is controlled and, if necessary, corrected during the electrical dimensioning in Section 4.5.

Furthermore, compression pads with a thickness of 1 mm are implemented after every other cell to absorb the mechanical stress caused by the breathing of the cells during charge-discharge cycles. Due to the very limited space available, the smallest current collector tabs available in the production system with a width of 15 mm are used.

4.4. Thermal Design and Dimensioning of the Cooling System. The in-plane thermal conductivity increases from $14 \text{ W}\cdot\text{m}^{-1}\cdot\text{K}^{-1}$ for the high-energy cell type to $37.3 \text{ W}\cdot\text{m}^{-1}\cdot\text{K}^{-1}$ for the high-power cell type. This increase originates from the growing fraction of highly thermally conductive current collector material considered in the parallel connection of the different layers. At the same time, the through-plane thermal conductivity is reduced from $0.56 \text{ W}\cdot\text{m}^{-1}\cdot\text{K}^{-1}$ to $0.37 \text{ W}\cdot\text{m}^{-1}\cdot\text{K}^{-1}$. Hereby, the increasing fraction of the separator with a very low thermal conductivity presents the bottle neck of the serial connection of the layers.

The temperature trajectory for the mountain trip load profile (Figure 8) is shown in Figure 10 for each of the five cell types. Hereby, an initial and ambient temperature of 25°C was assumed. Regarding the e-bike system, edge heat transfer was assumed and a constant heat transfer coefficient of $\alpha = 40 \text{ W}\cdot\text{m}^{-2}\cdot\text{K}^{-1}$ was applied at the outer surface of the

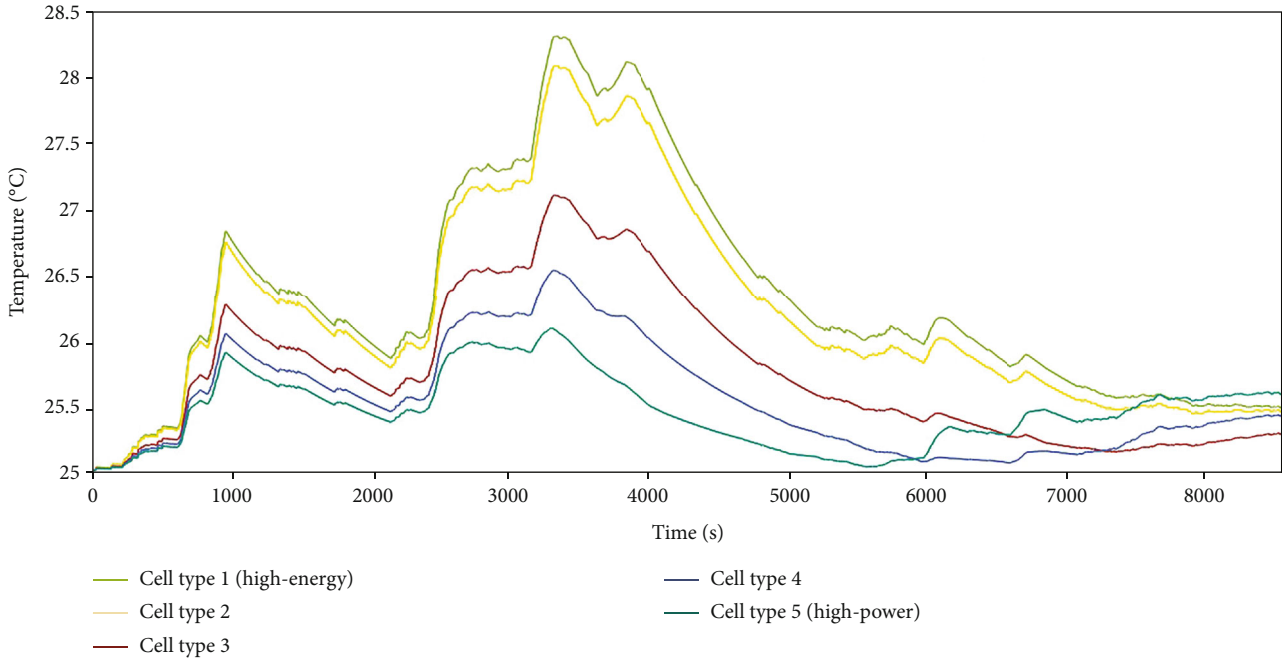


FIGURE 10: Comparison of the caloric mean temperature of the five cell types for the mountain trip load profile.

casing. Hereby, the in-plane thermal conductivity is most significant for the heat removal. In addition to the highest thermal conductivity, the high-power cell type 5 is also paired with the lowest internal resistance. Thus, the mean temperature and thermal gradient within the cells are lowest for the high-power cells. However, the temperature is sufficiently low in all of the cell types due to the small load applied; therefore, even cell type 1 with the highest energy content does not overheat.

Furthermore, the temperature increase for cell type 5 is comparatively high, starting at approx. 5500 s. The same applies to cell type 4 starting at approx. 6500 s. This behavior can be explained by the lower capacity of those cells due to the use of thinner active material layers. Consequently, the cells discharge faster when the same current is applied. Due to the higher internal resistance at lower states of charge, the amount of heat generated becomes higher and the temperature rises.

4.5. Selection of the Cell Type and a Wiring Topology. The mechanical layout of the 3p10s battery system (see Figure 9(b)) leads to the electrical topology depicted in Figure 11. One electrical cell connector links three negative and three positive tabs and therefore six cells to realize this topology. This cell connector is notionally split into five sections to calculate the ohmic resistance between two cells using a finite element method model.

The electrical model is used iteratively to determine first the best basic cell type and subsequently the most suitable connectors. The iterative electrical simulation starts with BCT 1 because it offers the highest energy density (see Figure 4). Considering the cell volume specified in Section 4.3, this leads to a cell capacity of 6.5 Ah. For the first simulation run, a 0.5 mm thick aluminum connector with a

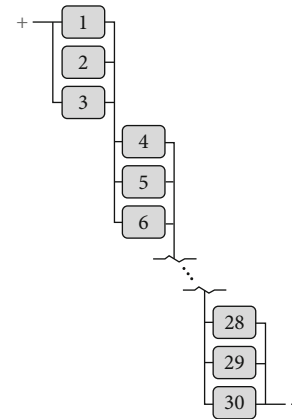


FIGURE 11: Graphical depiction of the 3p10s connection. Each box resembles one battery cell.

cell-to-cell connection resistance of 0.32 mΩ is chosen. Additionally, an electrical resistance of 0.16 mΩ for a laser weld to bond the cell tabs to the cell connectors is considered according to Brand et al. [43]. Figure 12(a) shows the current and SOC development for the last three cells of the battery system during the highest power demand of the load profile (see Figure 8). Cell 28 is subjected to the highest discharge current of -8.76 A or 1.35 C due to its position in the resistance arrangement. This is lower than the cell’s maximum discharge current of 5 C. According to the multiscale multidomain model [22], the cells can sustain this discharge current for two minutes, while the high current discharge pulses in the e-bike profile are shorter than ten seconds. BCT 1 therefore offers enough power for the e-bike application and is chosen for the following simulations.

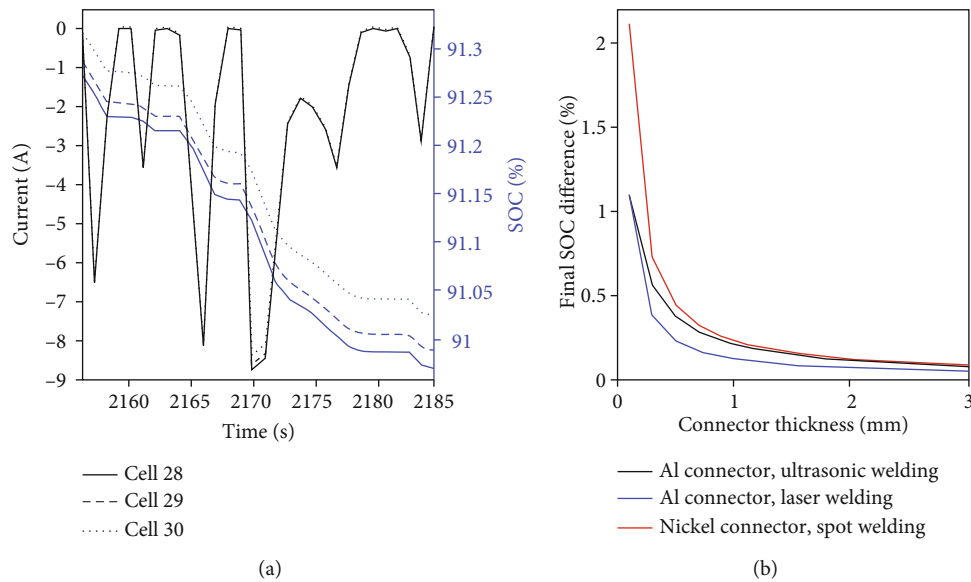


FIGURE 12: (a) The current and SOC development of the last three cells in the e-bike battery during the phase in the load profile with the highest power demand. The connection resistances resemble a 0.5 mm thick aluminum connector and laser welding. (b) Influence of cell connector thickness on the SOC difference at the end of the load cycle for different combinations of the cell connector material and the welding method.

In the next iterations, the components for the electrical connections are chosen. Important design goals for an e-bike battery are low weight and good high-volume manufacturability. This favors the use of aluminum for the connection elements due to its superior weight-conductivity ratio and low price. Aluminum forms an oxide layer at the surface and, therefore, requires ultrasonic welding or laser welding be joined with battery cell tabs [44]. Cell connectors made out of nickel enable cheaper spot welding and are therefore considered as third option. The finite element method model is used to calculate the ohmic resistances of aluminum and nickel connectors with thicknesses between 0.1 mm and 3 mm. The electrical resistance of the joint is defined at 0.32 m Ω for ultrasonic welding, 0.16 m Ω for laser welding, and 0.2 m Ω for spot welding. After one load profile is simulated, the SOC difference between the highest and lowest charged cell in the battery system is analyzed to choose a combination of material, welding method, and cell connector thickness. A high SOC difference leads to nonuniform aging as well as reduced usable capacity and power. Figure 12(b) shows the influence of the cell connector thickness on the final SOC difference for the three viable combinations of materials and welding methods. The system shows diminishing benefits when the cell connector thickness is increased above 1 mm. The combination of aluminum connectors and laser welds leads to the most uniform load distribution between the cells and is, therefore, chosen for the application.

4.6. Specification of the Safety Components. A metal housing made from aluminum is used for the battery pack to prevent mechanical abuse from outside and provide a frame for the bracing of the cells. Due to the small size and capacity of the single cells and, thus, the additional limited energy content of the whole system, thermal barriers between the cells are not used in this application.

Figure 13 displays simulated temperature curves and gas release rates of the 30 cells in the battery system. The simulation is set up with the results obtained from the previous design steps, using the thermal and chemical properties of basic cell type 1 and the geometry and arrangement, as shown in Figure 9. In the simulated scenario, thermal runaway is triggered in one cell by heating. The average temperature curves in Figure 13(a) show that it takes 22.28 min between the thermal runaway of the first and the last cell. Except for the triggered one, the cells reach a peak temperature of around 400°C.

Further, the simulation results in a total amount of gas of 377.6 L during this 30 min. The peak gas release is found to be 1.26 L/s (see Figure 13(b)). Therefore, as an additional safety measure, a safety valve can be chosen and dimensioned according to these results. Including a safety margin, a maximum flow rate of 2 L/s is recommended based on the simulation results.

4.7. Documentation and Transfer to the Production System. Assuming the same energy density on a unit cell level for both systems, our battery pack made from format-flexible cells obtains a 12% higher energy content than the original BOSCH system with approx. 700 Wh compared to 625 Wh.

After the design process is completed, the cell production line receives the instruction to produce 30 equal cells per system. Those are of BCT 1 with a cell capacity of 6.5 Ah. BCT 1 means that the cell has a porosity of 20% and a coating thickness of 131 μm for the cathode and a porosity of 21% and a coating thickness of 130 μm for the anode. The octagonal geometry and thickness of the cells of 11.1 mm are specified by tables, and the automatically generated construction drawing is shown in Figure 14(a). The tabs have a width of 15 mm and a thickness of 0.2 mm.

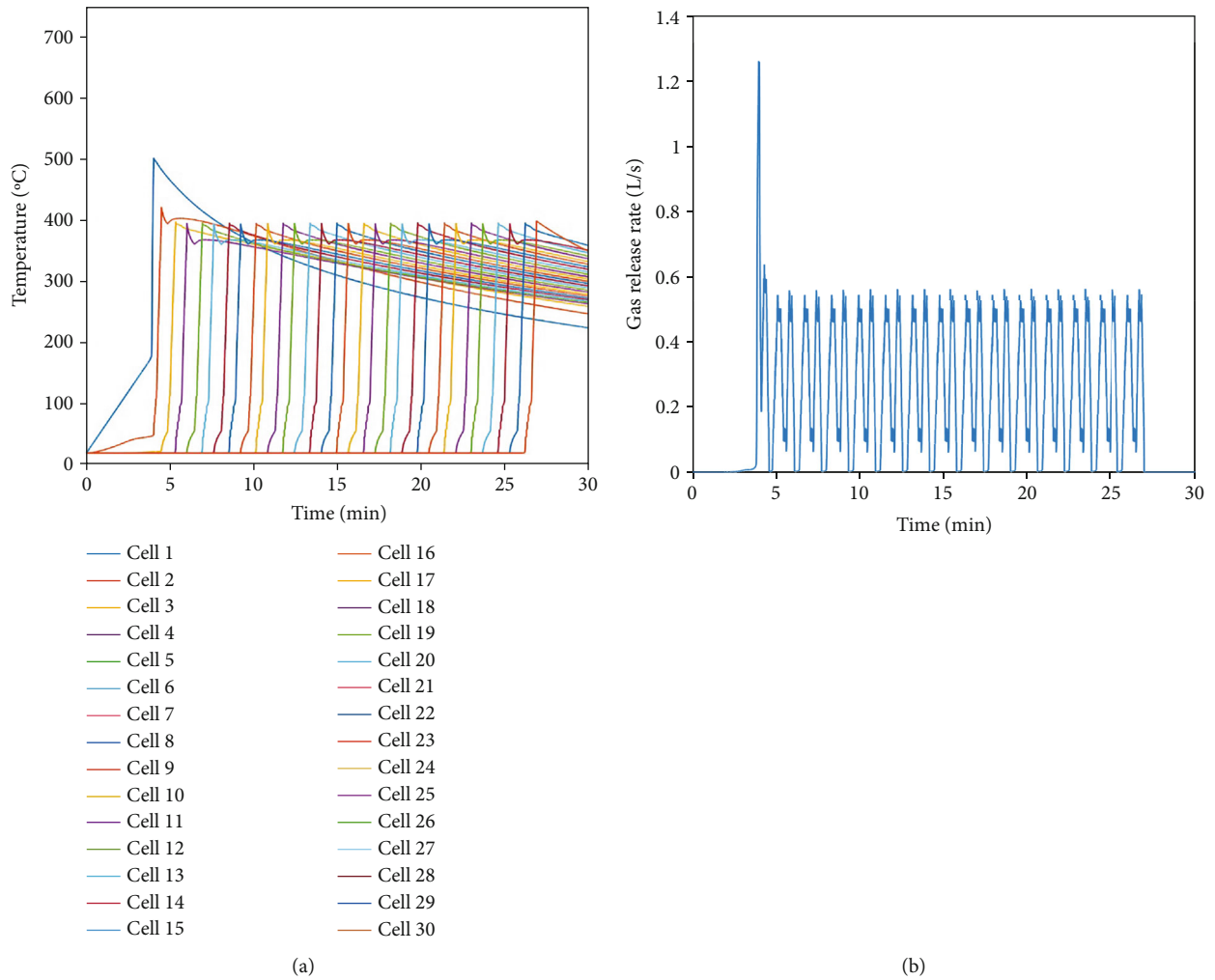


FIGURE 13: Simulation results of the battery system during a thermal event: (a) average temperature of the 30 cells and (b) gas release rate.

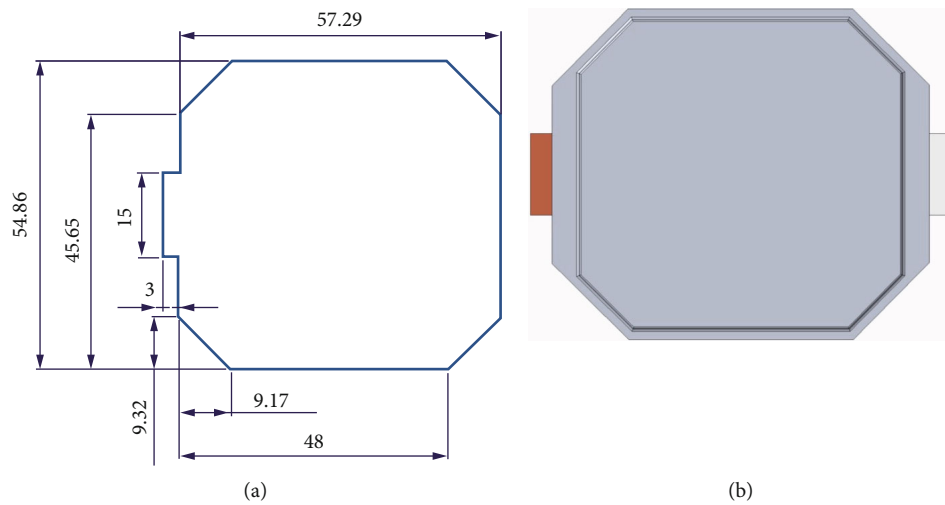


FIGURE 14: (a) Dimensions of a single electrode sheet and (b) CAD image of one cell used in the e-bike battery pack.

The 3p10s connection of the cells leads to a nominal system voltage of 36 V and a capacity of 19.5 Ah. The battery pack includes no active cooling system and no thermal barriers but compression pads after every other cell with a thickness of 1 mm in the braced state.

In addition to the depiction of the whole battery pack within the housing in Figure 9, the CAD image of a single cell is generated (Figure 14(b)) and deposited in the database as well.

5. Conclusions

We presented a new approach for the application-oriented design of the battery systems. In contrast to established procedure, this methodology does not improve the properties of a standard cell format but is based on format-flexible cells, i.e., with varying cell shapes to achieve higher energy and power densities on the battery system level. The core is a product-production codesign, which leverages synergies of an agile production line and the comprehensive design process. We show how the variety of combinations becomes manageable by defining the BCTs and establishing a toolkit. Furthermore, we structure the design process into consecutive steps that strongly interlock to lead to a holistically optimized battery system design. Thus, the tool introduced herein can be adjusted to the characteristics and limitations of the production system regarded and, thereby, enable a production-oriented product design.

Regarding the design of an e-bike battery pack, we showed a case study for the tool and gave more insight into the single design steps and interim results.

The method presented is applicable to various cell geometries, including triangular, trapezoidal, or even round shapes. A variation of the cell chemistry is not yet implemented but possible, as the whole tool is founded on physics-based simulation models that can handle different material systems—if parameterized accordingly.

Once the conventional self-imposed restrictions on battery systems, such as rectangular cell shapes or the use of only one cell chemistry within a system, are lifted, an enormous design space can be opened up. The design tool presented here is the first step in exploiting this potential.

Data Availability

The data used to support the findings of this study have not been made available because they are not relevant for the methodology described in this work.

Conflicts of Interest

The authors declare that there is no conflict of interest regarding the publication of this paper.

Authors' Contributions

J.G. and S.P. were responsible for the conceptualization. J.G., S.P., R.M., P.M., D.S., A.S., S.S., N.W., and Y.Z. were responsible for the methodology. J.G., R.M., P.M., D.S., A.S., P.S.,

N.W., and Y.Z. were responsible for the software. J.G., R.M., P.M., D.S., A.S., S.S., P.S., N.W., and Y.Z. were responsible for the validation. J.G., R.M., P.M., S.P., D.S., A.S., S.S., P.S., N.W., and Y.Z. were responsible for the formal analysis. T.W. was responsible for the resources. J.G. and S.P. wrote the original draft. J.G., S.P., R.M., P.M., D.S., A.S., S.S., P.S., N.W., Y.Z., and T.W. wrote, reviewed, and edited the manuscript. J.G., S.P., and P.M. were responsible for the visualization. T.W., J.G., and S.P. were responsible for the supervision. T.W. was responsible for the project administration. T.W. was responsible for the funding acquisition. All authors have read and agreed to the published version of the manuscript.

Acknowledgments

We thank our colleagues who are building and operating the production plant for their input and the great collaboration within the project. Furthermore, we want to thank Max Renaud (TVT) for the disassembly of the battery pack and Coboc GmbH & Co. KG for providing the exemplary load profiles. We acknowledge the support by the KIT Publication Fund of the Karlsruhe Institute of Technology. This research was funded by the Federal Ministry of Education and Research (grant number 03XP0369A) and the Ministry of Science, Research and Art of Baden-Württemberg (grant number 32-7533-4-161.2/9/12).

Supplementary Materials

A Supplementary Information to this article is available. (*Supplementary Materials*)

References

- [1] F. Degen, "Lithium-ion battery cell production in Europe: scenarios for reducing energy consumption and greenhouse gas emissions until 2030," *Journal of Industrial Ecology*, vol. 27, no. 3, pp. 964–976, 2023.
- [2] W. Appiah, J. Park, S. Song, S. Byun, M. H. Ryou, and Y. M. Lee, "Design optimization of $\text{LiNi}_{0.6}\text{Co}_{0.2}\text{Mn}_{0.2}\text{O}_2$ /graphite lithium-ion cells based on simulation and experimental data," *Journal of Power Sources*, vol. 319, pp. 147–158, 2016.
- [3] M. Astaneh, J. Andric, L. Löfdahl, and P. Stopp, "Multiphysics simulation optimization framework for lithium-ion battery pack design for electric vehicle applications," *Energy*, vol. 239, article 122092, 2022.
- [4] A. Epp and D. U. Sauer, "Multiperspective optimization of cell and module dimensioning for different lithium-ion cell formats on geometric and generic assumptions," *Energy Technology*, vol. 10, no. 3, article 2100874, 2022.
- [5] C. Bouvy, S. Ginsberg, P. Jeck, B. Hartmann, S. Baltzer, and L. Eckstein, "Holistic battery pack design," in *Proceedings of the 21st Aachen Colloquium Automobile and Engine Technology 2012*, Aachen, Germany, 2012.
- [6] A. Epp, R. Wendland, J. Behrendt, R. Gerlach, and D. U. Sauer, "Holistic battery system design optimization for electric vehicles using a multiphysically coupled lithium-ion battery design tool," *Journal of Energy Storage*, vol. 52, article 104854, 2022.
- [7] E. Gerlitz, D. Botzem, H. Weinmann, J. Ruhland, and J. Fleischer, "Cell-to-Pack-Technologie für Li-Ionen-Batterien,"

- Zeitschrift für wirtschaftlichen Fabrikbetrieb*, vol. 116, no. 10, pp. 689–694, 2021.
- [8] S. H. Ha, K. H. Shin, H. W. Park, and Y. J. Lee, “Flexible lithium-ion batteries with high areal capacity enabled by smart conductive textiles,” *Small*, vol. 14, no. 43, article e1703418, 2018.
 - [9] W. Li, “Electrochemical power systems for advanced driver-assistant vehicles,” in *Advanced Driver Assistance Systems and Autonomous Vehicles*, Y. Li and H. Shi, Eds., Springer, Singapore, 2022.
 - [10] P. K. D. Pramanik, N. Sinhababu, B. Mukherjee et al., “Power consumption analysis, measurement, management, and issues: a state-of-the-art review of smartphone battery and energy usage,” *IEEE Access*, vol. 7, pp. 182113–182172, 2019.
 - [11] J. Ruhland, T. Storz, F. Kößler et al., “Development of a parallel product-production co-design for an agile battery cell production system,” in *Towards Sustainable Customization: Bridging Smart Products and Manufacturing Systems. CARV MCPC 2021*, Lecture Notes in Mechanical Engineering, A. L. Andersen, Ed., Springer, Cham, 2021.
 - [12] J. Fleischer, F. Fraider, F. Kößler, D. Mayer, and F. Wirth, “Agile production systems for electric mobility,” in *Procedia CIRP 107*, Lugano, Switzerland, 2022.
 - [13] S. Grabmann, M. K. Kick, C. Geiger, F. Harst, A. Bachmann, and M. F. Zaeh, “Toward the flexible production of large-format lithium-ion batteries using laser-based cell-internal contacting,” *Journal of Laser Applications*, vol. 34, no. 4, p. 42017, 2022.
 - [14] CUSTOMCELLS, “Advanced battery cell development and production. Better for any application—specialties in series,” September 2023, https://www.customcells.de/fileadmin/user_upload/CUSTOMCELLS-Broschure_01.pdf.
 - [15] S. Henschel, F. Kößler, and J. Fleischer, “Material flow of an agile battery cell production system based on diffusion-tight transport boxes and driverless transport systems,” in *Production at the Leading Edge of Technology. WGP 2023*, Lecture notes in production engineering, T. Bauernhansl, A. Verl, M. Liewald, and H. C. Möhring, Eds., Springer, Cham, 2024.
 - [16] L. Overbeck, S. Voigtländer, and G. Lanza, “Optimal line configurations for agile production systems for battery cell manufacturing,” *Procedia CIRP*, vol. 118, pp. 976–981, 2023.
 - [17] Tech Times, September 2023, <https://www.techtimes.com/articles/254392/20201122/ifixit-reveals-iphone-12-pro-max-sl-shaped-battery-internal.html>.
 - [18] LG Chem, September 2023, <https://www.lgchem.com/global/lg-chem-history/timeline>.
 - [19] Old Cars Weekly, September 2023, <https://www.oldcarsweekly.com/features/car-of-the-week-1923-ford-model-t-express-pickup>.
 - [20] S. aus der Wiesche, “Industrial thermoforming simulation of automotive fuel tanks,” *Applied Thermal Engineering*, vol. 24, no. 16, pp. 2391–2409, 2004.
 - [21] C. Lensch-Franzen, M. Gohl, M. Schmalz, and T. Doguer, “Von der Zelle zum Batteriesystem - Verschiedene Zellformate und ihre Systemintegration,” *MTZ - Motortechnische Zeitschrift*, vol. 81, no. 11, pp. 70–75, 2020.
 - [22] A. Schmidt, D. Oehler, A. Weber, T. Wetzels, and E. Ivers-Tiffée, “A multi scale multi domain model for large format lithium-ion batteries,” *Electrochimica Acta*, vol. 393, p. 139046, 2021.
 - [23] H. Bockholt, M. Indrikova, A. Netz, F. Golks, and A. Kwade, “The interaction of consecutive process steps in the manufacturing of lithium-ion battery electrodes with regard to structural and electrochemical properties,” *Journal of Power Sources*, vol. 325, pp. 140–151, 2016.
 - [24] V. Laue, F. Röder, and U. Krewer, “Joint structural and electrochemical modeling: impact of porosity on lithium-ion battery performance,” *Electrochimica Acta*, vol. 314, pp. 20–31, 2019.
 - [25] M. J. Lain, J. Brandon, and E. Kendrick, “Design strategies for high power vs. high energy lithium ion cells,” *Batteries*, vol. 5, no. 4, p. 64, 2019.
 - [26] P. Müller-Welt, K. Nowoseltschenko, K. Bause, and A. Albers, “A methodology for application-specific concept definition of battery systems using pouch cells produced in flexible format,” in *35th International Electric Vehicle Symposium and Exhibition (EVS35)*, Oslo, Norway, June 2022.
 - [27] P. Müller-Welt, K. Nowoseltschenko, C. Garot, K. Bause, and A. Albers, “Automated optimization of a cell assembly using format-flexibly produced pouch cells,” in *22. Internationale Stuttgarter Symposium*, Stuttgart, Germany, March 2022.
 - [28] G. Offer, Y. Patel, A. Hales, L. Bravo Diaz, and M. Marzook, “Cool metric for lithium-ion batteries could spur progress,” *Nature*, vol. 582, no. 7813, pp. 485–487, 2020.
 - [29] X. M. Xu and R. He, “Research on the heat dissipation performance of battery pack based on forced air cooling,” *Journal of Power Sources*, vol. 240, pp. 33–41, 2013.
 - [30] J. Wang, S. Lu, Y. Wang, C. Li, and K. Wang, “Effect analysis on thermal behavior enhancement of lithium-ion battery pack with different cooling structures,” *Journal of Energy Storage*, vol. 32, article 101800, 2020.
 - [31] Y. Huo, Z. Rao, X. Liu, and J. Zhao, “Investigation of power battery thermal management by using mini-channel cold plate,” *Energy Conversion and Management*, vol. 89, pp. 387–395, 2015.
 - [32] M. S. Patil, J.-H. Seo, S. Panchal, S.-W. Jee, and M.-Y. Lee, “Investigation on thermal performance of water-cooled Li-ion pouch cell and pack at high discharge rate with U-turn type microchannel cold plate,” *International Journal of Heat and Mass Transfer*, vol. 155, p. 119728, 2020.
 - [33] S. Wang, S. Ji, and Y. Zhu, “A comparative study of cooling schemes for laminated lithium-ion batteries,” *Applied Thermal Engineering*, vol. 182, article 116040, 2021.
 - [34] Q. Queisser, L. Cloos, F. Boehm, D. Oehler, and T. Wetzels, “Impact of the level of homogenization in 3D thermal simulation on the internal temperature distribution of li-ion battery cells,” *Energy Technology*, vol. 9, no. 6, article 2000915, 2021.
 - [35] D. Werner, A. Loges, D. J. Becker, and T. Wetzels, “Thermal conductivity of Li-ion batteries and their electrode configurations – a novel combination of modelling and experimental approach,” *Journal of Power Sources*, vol. 364, pp. 72–83, 2017.
 - [36] A. Kersten, M. Kuder, W. Han et al., “Online and on-board battery impedance estimation of battery cells, modules or packs in a reconfigurable battery system or multilevel inverter,” in *IECON 2020 The 46th Annual Conference of IEEE Industrial Electronics Society*, pp. 1884–1891, Singapore, October 2020.
 - [37] P. V. Chombo and Y. Laoonual, “A review of safety strategies of a Li-ion battery,” *Journal of Power Sources*, vol. 478, p. 228649, 2020.
 - [38] X. Feng, D. Ren, X. He, and M. Ouyang, “Mitigating thermal runaway of lithium-ion batteries,” *Joule*, vol. 4, no. 4, pp. 743–770, 2020.
 - [39] X. Feng, X. He, M. Ouyang et al., “Thermal runaway propagation model for designing a safer battery pack with 25 Ah LiNi_xCo_yMn_zO₂ large format lithium ion battery,” *Applied Energy*, vol. 154, pp. 74–91, 2015.

- [40] C. Yuan, Q. Wang, Y. Wang, and Y. Zhao, "Inhibition effect of different interstitial materials on thermal runaway propagation in the cylindrical lithium-ion battery module," *Applied Thermal Engineering*, vol. 153, pp. 39–50, 2019.
- [41] N. Weber, S. Schuhmann, J. Tübke, and H. Nirschl, "Chemical thermal runaway modeling of lithium-ion batteries for prediction of heat and gas generation," *Energy Technology*, vol. 11, no. 10, article A6220, 2023.
- [42] BOSCH: packed with power, "BOSCH eBike batteries," November 2023, <https://www.bosch-ebike.com/us/products/batteries>.
- [43] M. J. Brand, E. I. Kolp, P. Berg, T. Bach, P. Schmidt, and A. Jossen, "Electrical resistances of soldered battery cell connections," *Journal of Energy Storage*, vol. 12, pp. 45–54, 2017.
- [44] S. S. Lee, T. H. Kim, S. J. Hu, W. W. Cai, and J. A. Abell, "Joining technologies for automotive lithium-ion battery manufacturing: a review," in *Proceedings of the ASME 2010 International Manufacturing Science and Engineering Conference. ASME 2010 International Manufacturing Science and Engineering Conference, Volume 1*, pp. 541–549, Erie, Pennsylvania, USA, October 2010.